

Significantly Enhanced Photocatalytic Hydrogen Evolution over Cu₂O Embedded on TiO₂ Aerogels under Simulated Solar Light Irradiation

Liang Jiang¹, Kexin Wang¹, Ziyu Zeng¹, Wei Wang¹, Jiao He¹
and Jiaqiang Wang^{1*}

¹School of Chemical Sciences and Technology, National Center for International Research on Photoelectric and Energy Materials, School of Materials and Energy, Yunnan University, Kunming-650091, People's Republic of China.

Authors' contributions

This work was carried out in collaboration among all authors. Author LJ designed the study, performed the statistical analysis, wrote the protocol, and wrote the first draft of the manuscript. Authors KW and ZZ managed the analyses of the study. Authors WW, JH managed the literature searches. All authors read and approved the final manuscript.

Article Information

Editor(s):

(1) Dr. Madogni Vianou Irene, Universite d'Abomey-Calavi, Benin.

Reviewers:

(1) Yuan Yao, Ocean University Of China, China.

(2) Chenchen Zhao, Public university in Harbin, China.

Complete Peer review History: <https://www.sdiarticle4.com/review-history/70839>

Original Research Article

Received 01 June 2021
Accepted 03 August 2021
Published 09 August 2021

ABSTRACT

A high surface area mesoporous Cu₂O embedded on TiO₂ (Cu₂O-TiO₂) aerogel was prepared and used in photocatalytic splitting of water under simulated solar light irradiation. Highly efficient hydrogen production was achieved over 3 wt% Cu₂O-modified TiO₂ aerogel photocatalyst with a high rate of 1.40 mmol/(g·h) under simulated solar irradiation. The hydrogen production efficiency of 3 wt% Cu₂O-modified TiO₂ aerogel was about 33 and 9 times higher than those of pure TiO₂ aerogels (0.043 mmol/g·h) and Cu₂O-modified commercial TiO₂, Degussa P25 (0.15 mmol/g·h) with the same ratio, respectively. For comparison, no hydrogen was detected when Cu₂O was used alone as the catalyst, and the activity of Cu₂O mechanically mixed TiO₂ aerogel with the same ratio was 13 times lower than Cu₂O-TiO₂ aerogel. This result implied that the Cu₂O loading was benefit to promote the separation and migration of electron-hole pair. Furthermore, the Cu₂O loading enhanced the absorbance in 300-800 nm region as compared to pure TiO₂ aerogel. Cu₂O-

*Corresponding author: Email: jqwang@ynu.edu.cn;

TiO₂ aerogels have very high specific surface area (400-500 m²/g) and good recyclability for at least 3 cycles, which suggests that the materials have promising prospects in photocatalytic hydrogen production.

Keywords: Cu₂O; TiO₂ aerogels; hydrogen evolution; solar-light-activated; photocatalysis.

1. INTRODUCTION

In view of increasingly serious energy and environmental problems, photocatalytic hydrogen production from water splitting has attracted great attention since hydrogen has been identified as a promising fuel for sustainable energy supply [1-3]. Most of the semiconductor materials reported in the literature as photocatalysts are based on TiO₂ [4-9]. Unfortunately, the photocatalytic hydrogen production efficiency involving TiO₂ alone was relatively low [10-13]. Many approaches have been investigated to improve the hydrogen production rate of TiO₂ [14-16]. For example, hybrid TiO₂ and Cu_xO systems have been used to photocatalyze hydrogen evolution [17-22]. In particular, Cu₂O/TiO₂ composite has been found to exhibit high hydrogen evolution yield under the solar light irradiations since Cu₂O is one of the few p-type direct band gap semiconductors [21, 23-28].

Recently, aerogels consisting of open and highly porous structure have attracted great attention in various applications [29,30]. However, the study of photocatalytic hydrogen production from water splitting on aerogels was still very limited [31-35]. Given the aforementioned photoactivities and porosity of titania aerogels and enhancement of Cu₂O cocatalyst performance, we may expect that integration of TiO₂ aerogels and Cu₂O cocatalyst would adopt their merits in photocatalysis. Herein Cu₂O embedded on TiO₂ aerogels (Cu₂O-TiO₂) were synthesized, and used in photocatalytic splitting of water under solar light irradiation. It is demonstrated in this research that the photocatalytic activity of Cu₂O-TiO₂ aerogels for hydrogen evolution under solar light is significantly enhanced in comparison with pure TiO₂. Furthermore, the photostability of composites and the effects of Cu₂O content on the specific surface area and the photocatalytic activity of Cu₂O-TiO₂ aerogels were also investigated.

2. EXPERIMENTAL DETAILS

All reagents were of analytical grade (purchased from Aladdin-Holdings Group, China) and were

used without further purification. Distilled water was used in all experiments.

2.1 Synthesis of Catalysts

2.1.1 Preparation of TiO₂ aerogels

TiO₂ aerogel was synthesized with a process modified from ref. [36]. A mixture of 20.0 mL (0.2713mol) acetone (CH₃COCH₃, 99%) and 0.54 mL (5.3 mmol) acetylacetone (CH₃COCH₂COCH₃, 99%) was added into 6.0 grams (24.07 mmol) of tetrabutyl titanate (Ti(OC₄H_{9-n})₄, 99%) under stirring. Then a mixture of acetone (7.6 mL) and water (1.2 mL) was added dropwise to form a solution which gradually transformed into a wet-gel. After aging at room temperature for 24 h, the gel was placed in a 50 mL autoclave and acetone was added until 80% of the volume of the autoclave was filled. The autoclave was heated at 313 K to form a crystalline TiO₂ wet-gel, which was then dried at room temperature for 4 h, 323 K for 4 h, 373 K for 2 h and 393 K for 2 h at atmospheric pressure to obtain the crystalline aerogels.

2.1.2 Preparation of Cu₂O-TiO₂ aerogels

The Cu₂O-TiO₂ aerogels were prepared by impregnation method [30, 31]. In a typical synthesis, TiO₂ aerogel (1.0 g) was dispersed in distilled water (80 mL), and then a certain volume of Cu(NO₃)₂·3H₂O aqueous solution (0.05 M) was added. The weight percentages of Cu₂O in the photocatalyst samples were 0, 1, 3, 5, 7 and 10; the resulting samples were labeled as CT_x, where x =0, 1, 3, 5, 7 and 10, respectively. Also, pure Cu₂O sample was prepared without the TiO₂ aerogel. The mixed solutions were stirred for 2 h at room temperature. After that, the suspensions were heated at 373 K for 12 h to remove water. Finally, the solid samples were calcined at 523 K for 4 h in air. We also prepared two samples for comparison. Cu₂O-P25 was prepared with the same method as CT₃ but replaced the TiO₂ aerogel by P25. According to weight percentages of Cu₂O in CT₃, the 3 wt% Cu₂O mixed TiO₂ aerogel was prepared by mechanical mixing method using the pure Cu₂O and TiO₂ aerogel.

2.1.3 Characterization of photocatalysts

Scanning electron microscopy (SEM) images of the samples were taken on a FEI Quanta 200FEG microscope. Pore size distributions, BET surface areas, and pore volumes were measured by nitrogen adsorption/desorption using a NOVA2000e gas sorption analyzer (Quanta chrome Corp). Prior to the analysis, the samples were degassed at 423 K for 1 h. X-ray powder diffraction (XRD) experiments were conducted on a D/max-3B spectrometer with Cu K_{α} radiation. Scans were made in the 2θ range: 283-363 K with a scan rate 283 K/min (wide angle diffraction). X-ray photoelectron was performed on a PHI5500ESCA analyzer. The main parameters were as follows: Mg K_{α} , 200 W, vacuum $\sim 10^{-7}$ Pa. High-resolution transmission electron microscopy (HRTEM) images were taken on a TEM (TECNAL G2S-TWIN F20). UV-Vis diffuse reflectance spectra (DRS) were measured on a Shimadzu UV-2401PC photometer. X-ray Photoelectron Spectroscopy (XPS) were in an ultrahigh vacuum chamber with a base pressure below 2.66×10^{-7} Pa at room temperature. Photoemission spectra were recorded by a Thermo fisher Scientific spectrometer (K-Alpha⁺) equipped with standard monochromatic Al K_{α} excitation source. All binding energies were referenced to C_{1s} at 284.8 eV.

2.1.4 Photocatalytic hydrogen production

The photocatalytic hydrogen evolution by water splitting was performed in a glass reaction cell with quartz cover connected to a closed gas circulation. 50 mg photocatalysts was dispersed in 100 mL of 10 vol % methanol aqueous solutions. And the suspension was exposed to a 300W Xe lamp equipped. Then the reaction solution was stirred continuously and cooled to room temperature by a flow of water. The amount of hydrogen evolved was determined at an interval of 1 h with online gas chromatography.

2.2 The Reproducibility of Photocatalysts

The recyclability study was carried out 3 times in order to determine the stability of the photocatalyst. Each test was carried out as described above for 5 hours under simulated solar light irradiation. After each test was completed, the gaseous products were evacuated from the reactor, and the material was centrifuged, then washed with deionized water and filtered. After dried at 343 K, the material was reused in reactor for hydrogen generation.

3. RESULTS AND DISCUSSION

3.1 Characterizations

Table 1 summarized the textural properties of all the materials. All the Cu_2O - TiO_2 aerogels have high surface areas (400-500 m^2/g). The surface areas, average pore size and pore volumes of the Cu_2O - TiO_2 aerogels are lower than those of CT0, which can be due to the pore blockage induced by Cu_2O loadings. The enhancement in H_2 production may be attributed to the high dispersion of catalyst in methanol aqueous solution and the high specific surface area of Cu_2O - TiO_2 aerogels. SEM and high-resolution TEM images of Cu_2O - TiO_2 aerogels are shown in Fig. 1(a), (b), (c) and (d), respectively. SEM reveals that this sample has no regular morphology and aggregated (Fig. 1 (a-b)). Fig. 1 (c-d) shows that the aggregated nanocrystal is composed of disordered primary nanoparticles (20-30 nm in size).

Fig. 2 shows the XRD patterns of the CTx samples with x varying from 0 to 10 in comparison to the pattern of Cu_2O . It is seen only anatase phase of TiO_2 were observed CT0 and Cu_2O - TiO_2 aerogel photocatalysts. No characteristic diffraction peaks of Cu_2O were observed due to the low content of Cu_2O and weak crystallization.

Table 1. Summary of textural properties of all the Cu_2O - TiO_2 aerogel samples

Sample	Brunner-Emmet-Teller (BET) measurements (m^2/g)	Pore volume (cm^3/g)	Pore diameter (nm)
CT0	507.8	1.25	9.9
CT1	483.4	1.09	8.9
CT3	471.3	1.16	9.5
CT5	406.6	0.96	8.2
CT7	451.7	0.91	9.0
CT10	438.3	0.92	8.3

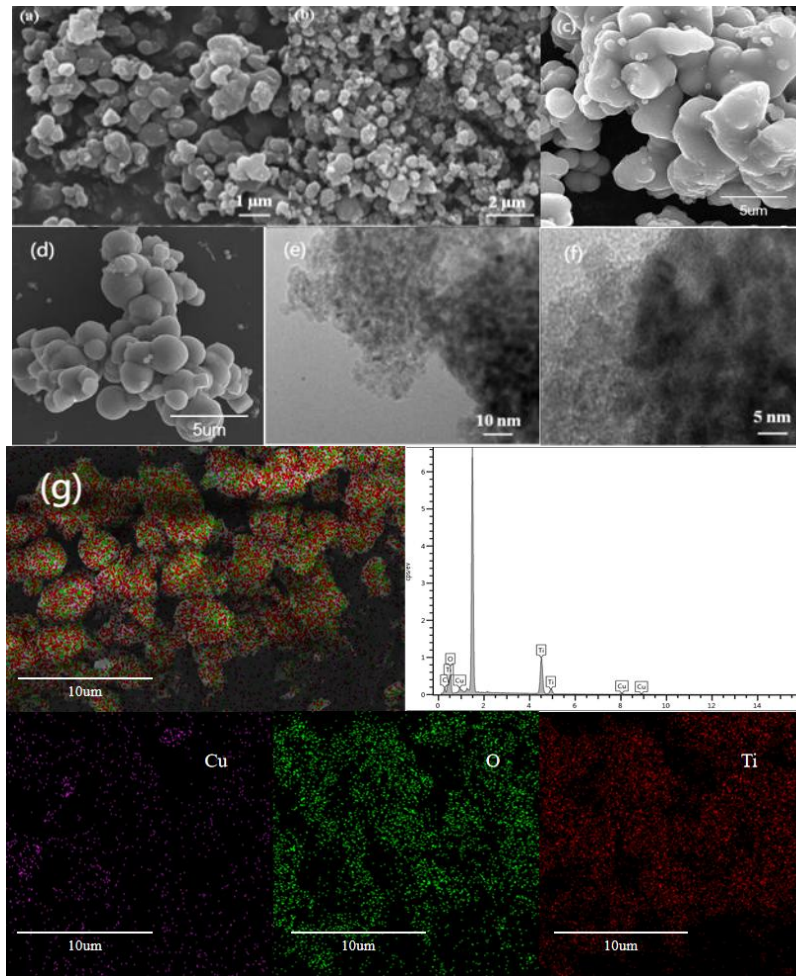
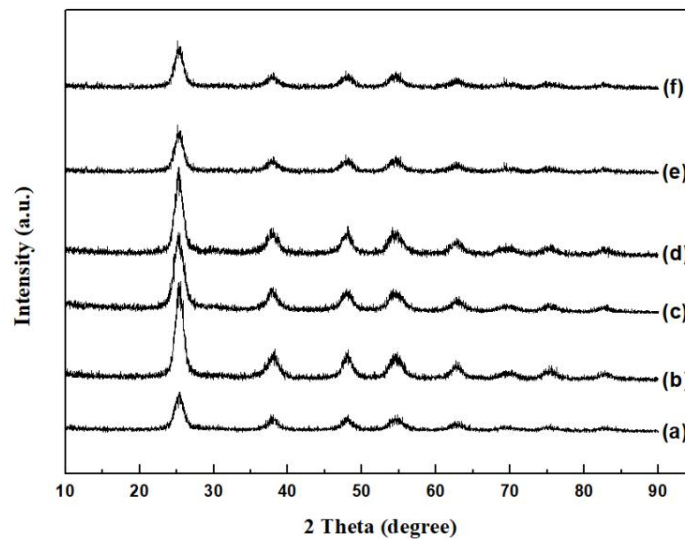


Fig. 1. SEM of (a-b) Cu₂O-TiO₂ aerogel with different crystal sizes, (c) TiO₂ aerogel, (d) Cu₂O, HRTEM images (e-f) of CT3, (g) SEM-EDS mapping of CT3



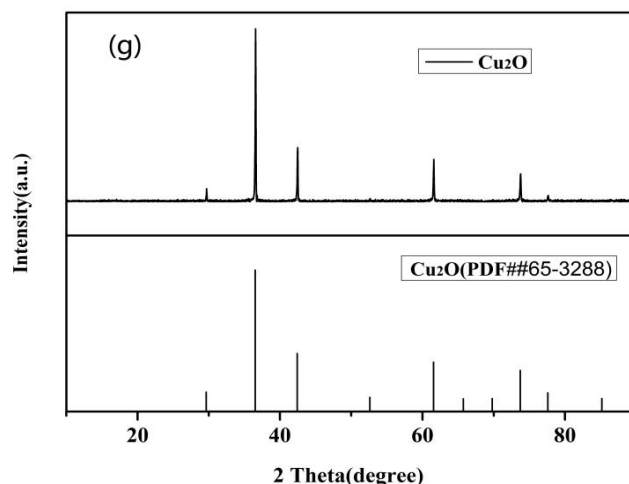


Fig. 2. X-ray diffraction pattern of (a) CT0, (b) CT1, (c) CT3, (d) CT5, (e) CT7, (f) CT10, (g)Cu2O

To further confirmed the existence of Cu_2O , X-ray photoelectron spectroscopy (XPS) measurements analysis of CT3 aerogel sample was performed, and the survey spectrum and high-resolution scans are shown in Fig. 3. In Fig. 3(a), Cu, Ti and O photoelectron lines from the sample were detected along with C peaks. In Fig. 3(b), Cu $2p_{3/2}$ spin orbital splitting photoelectrons were located at binding energies of 932.03 eV, and were assigned to the compound of Cu_2O [37-39]. By comparing the peak change of Ti in the Fig. 3(c), we can see that the binding energy of Ti in the doped composite material is 0.1 electron volts higher than that of the pure titanium dioxide aerogel.

Fig. 4 displays the UV-vis diffuse reflection spectra of the samples. A significant increase in the absorption at wavelengths shorter than 400 nm can be assigned to the intrinsic band gap absorption of TiO_2 [36]. The UV-vis spectra of CT3 with Cu_2O loading exhibit obviously enhanced absorption in the 300-800 nm region compared with that of pure TiO_2 aerogel (CT0). The absorption edge of CT3 obviously shifts to the visible-light region in comparison to CT0, implying that the prepared samples may have photocatalytic activity under simulated solar irradiation.

3.2 Photocatalytic H_2 Production Activity

Fig. 5 and Fig. 6 show the comparison of the photocatalytic H_2 production activity of the samples. As observed from Fig. 5, the content of Cu_2O has significant influence on the photocatalytic activity of TiO_2 aerogels. With the increasing Cu_2O content loaded on TiO_2 aerogel,

the photocatalytic activities increased initially while it decreased later. (Fig. 5a). It is probably due to the pore blockage and the reduction of active sites induced by the increasing Cu_2O content. As shown in Fig. 5b, CT3 shows the highest photocatalytic H_2 production efficiency (1.40 mmol/(g·h)), which exceeds that of CT10 (0.54 mmol/(g·h)) about 2.6 times.

We also studied the photocatalytic efficiency of CT0, Cu_2O -P25, 3 wt% Cu_2O mixed TiO_2 aerogel and Cu_2O for comparison (Fig. 6). The photocatalytic efficiency for CT3 is about 33, 9, and 13 times higher than those of CT0, Cu_2O -P25 and 3 wt% Cu_2O mixed TiO_2 aerogel, respectively (Fig. 6b). No hydrogen was detected when Cu_2O alone was used as the catalyst, suggesting that pure Cu_2O was not active for photocatalytic hydrogen production under the experimental conditions studied (Fig. 6a). The sample CT0 exhibited a very low photocatalytic activity owing to the rapid recombination between CB electrons and VB holes in TiO_2 aerogels [36]. The sample prepared by mechanical mixing method (3 wt% Cu_2O mixed TiO_2 aerogel) exhibited higher photocatalytic hydrogen production activity than CT0 and pure Cu_2O . However, its activity is still 13 times lower than CT3. This suggests that the loading of Cu_2O was benefit to promote the electron transfer and reduce the recombination of electron-hole pair [37]. Due to the matching of the band gap structure between Cu_2O and TiO_2 , photogenerated electrons could transfer from the conduction band of copper oxides to TiO_2 , while the holes at the valence band of TiO_2 might move to that of copper oxides [21,22].

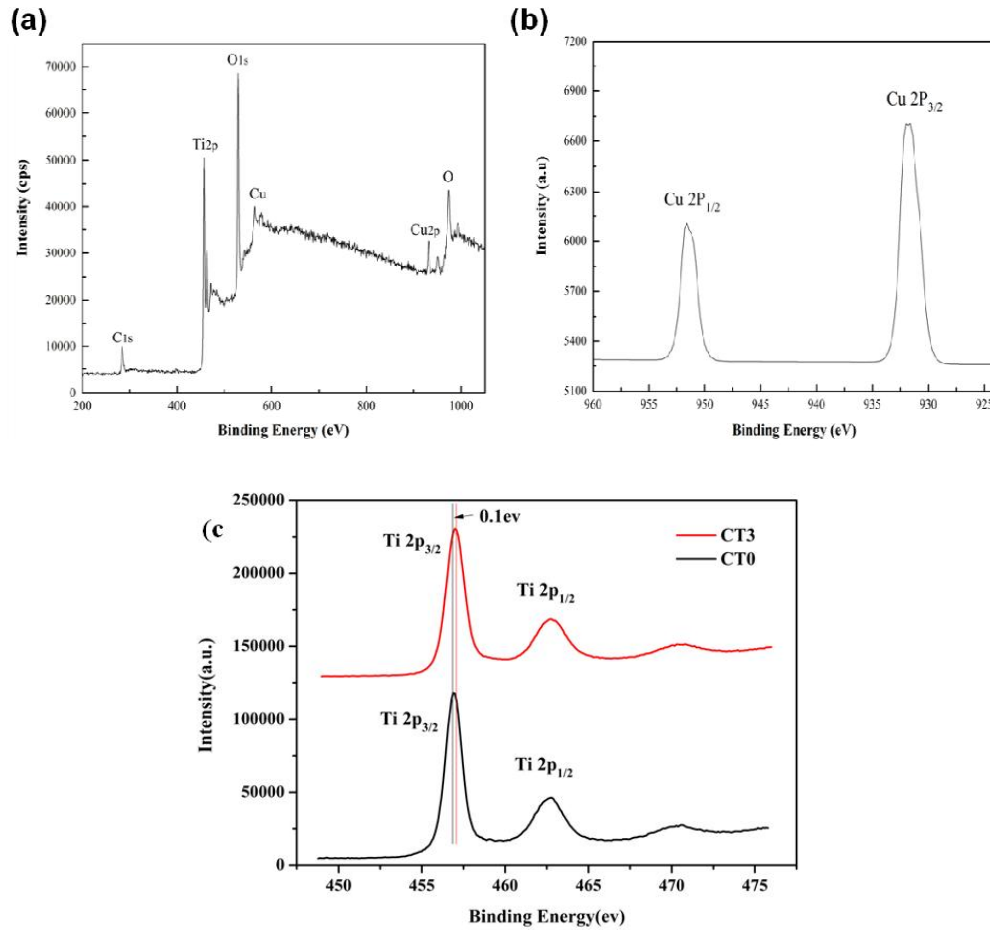


Fig. 3. (a) XPS survey spectrum of 3 wt% Cu₂O-TiO₂ aeroge photocatalyst, (b) High resolution Cu 2p spectrum, (c) Comparison of high-resolution spectra of Ti before and after doping

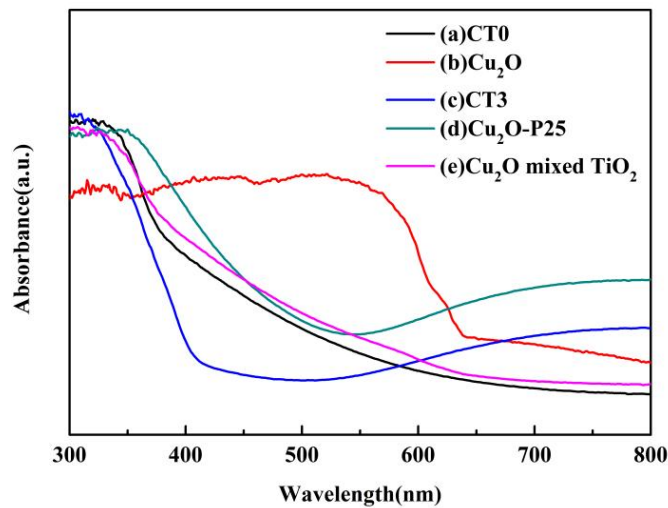


Fig. 4. UV-Vis spectra of , (a) CT0, (b) Cu₂O, (c) CT3, (d) Cu₂O-P25, (e)Cu₂O mixed TiO₂

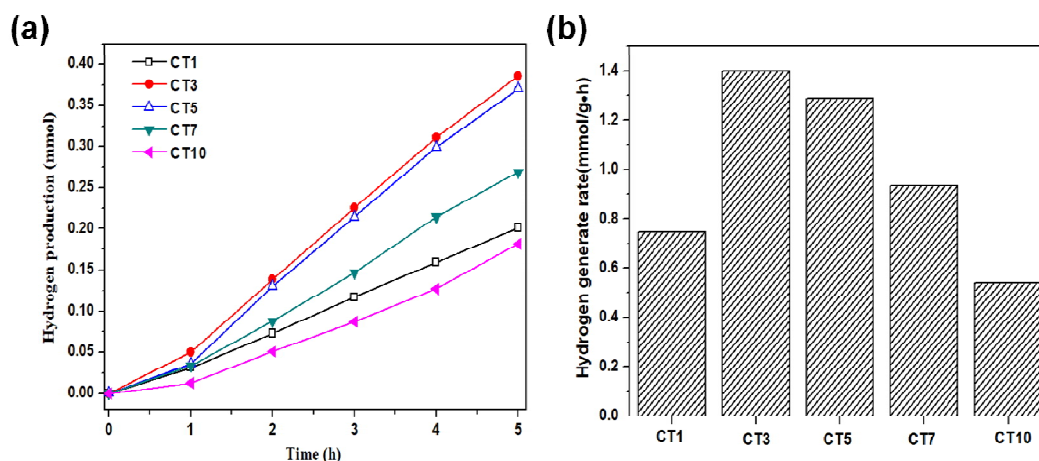


Fig. 5. Comparison of H₂ production and H₂ production efficiency over CT1, CT3, CT5, CT7 and CT10

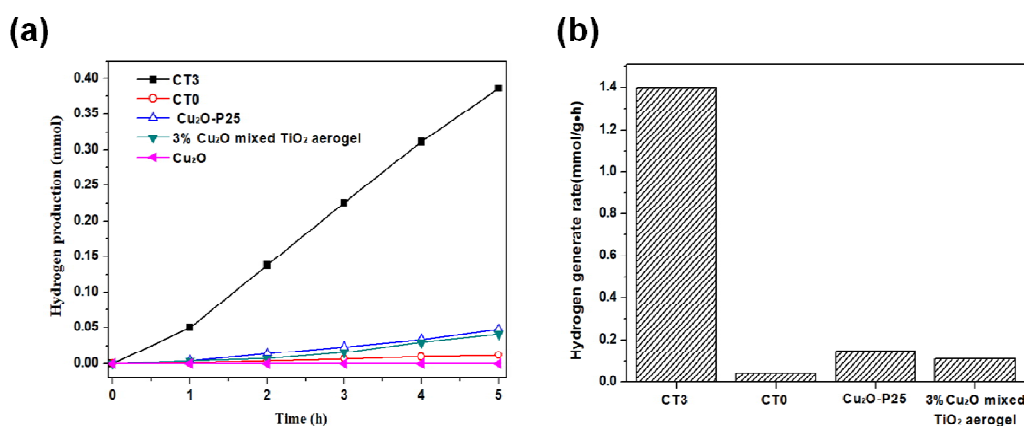


Fig. 6. Comparison of H₂ production and H₂ production efficiency over CT3, CT0, Cu₂O-P25, 3 wt% Cu₂O mixed TiO₂ aerogel, and Cu₂O

3.3 Possible Mechanism for the Enhanced Photocatalytic H₂ Production Activity

The result of UV-vis diffuse reflectance spectra implied that the Cu₂O loading enhanced the absorbance in 300-800 nm region as compared to pure TiO₂ aerogel. On the other hand, the conduction band edge of TiO₂ is higher than that of Cu₂O. The conduction band edge of Cu₂O has a less negative potential than H⁺/H₂ potential [38]. This facilitates the interfacial electron transfer from Cu₂O to H⁺ in the solution. Under simulated solar irradiation, TiO₂ and Cu₂O were activated at the same time. Photogenerated electrons transfer from the conduction band of TiO₂ into Cu₂O, and

accumulate at their lower conduction bands, while holes accumulate at the valence band of TiO₂ and Cu₂O [39]. Consequently, the photogenerated electron in Cu₂O can effectively reduce the protons to form H₂. Obviously, the quantum size effects increase the band gap in Cu₂O and also shift the conduction band to facilitate the transfer of photogenerated electrons. Although Cu₂O was activated by the light, photogenerated electrons could still be transferred from the conduction band of TiO₂ into that of Cu₂O, which resulted in a low activity of the sample CT1. In fact, the conduction band of bulk Cu₂O is less negative and may not allow for direct transfer of electrons from Cu₂O to H⁺ in the solution [40]. Therefore, with increasing Cu₂O content up to 3 wt%, the number of the Cu₂O

formed on the titania surface increases, resulting in the increase of its photocatalytic activity. However, when Cu₂O is higher than 3 wt%, a further increase in the Cu₂O content results in the reduction or disappearance of the quantum confinement effect, causing a decrease of the photocatalytic activity.

According to the absorption spectrum, use the Tauc-plot formula to convert the absorption spectrum:

$$\alpha h\nu^{1/n} = A(h\nu - E_g)(1)$$

In formula (1): α is the absorption coefficient, h is Planck's constant; ν is the optical frequency, n is a constant, direct band gap semiconductor $n=1/2$, indirect band gap semiconductor $n=2$. Use formula (1) to calculate the band gap and draw a tangent to the absorption cut-off edge, the results are shown in Table 1. CT3 has the narrowest band gap, which is 1.52 eV.

In the analysis of transient photocurrent response, the stronger the photocurrent, the higher the photogenerated carrier separation efficiency. It can be clearly seen from Fig 8(a)

that Cu₂O-TiO₂ has a fast photocurrent response under light conditions. It is worth noting that the photocurrent density of CT3 is significantly stronger than that of other composite materials. This is because the doping of Cu₂O enhances the generation and separation of photogenerated carriers, and the doping of 3wt% shows the strongest transient state Photocurrent.

Electrochemical impedance (EIS) is another effective electrochemical method to reveal the transfer and separation efficiency of electrons on the electrode. The study believes that a small EIS arc radius indicates that the charge transfer resistance between the working electrode and the electrolyte solution is small. The electrode has a more effective photo-generated charge transfer capability. As shown in Figure 8(b), compared with other materials, the EIS arc radius of CTx decreases with the increase of Cu₂O content, and the arc radius is minimized in CT3.

As the weight percentage of Cu₂O increases, the arc radius becomes larger, which further shows that Cu₂O doping enhances the separation and transfer of photogenerated electron-hole pairs.

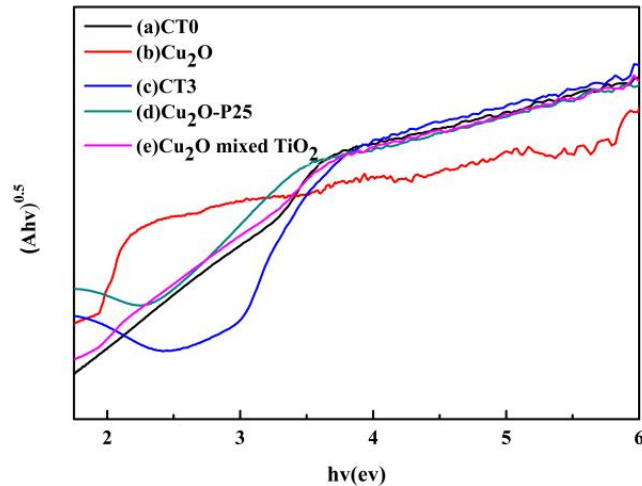


Fig. 7. $(Ah\nu)^{0.5}$ and $h\nu$ relationship diagram of (a) CT0, (b) Cu₂O, (c) CT3, (d) Cu₂O-P25, (e) Cu₂O mixed TiO₂

Table 2. Absorption band edge and band width of composite materials

Sample	Absorption band edge λ (nm)	Band gap E_g (eV)
CT0	659.6	1.78
Cu ₂ O	715.9	1.64
CT3	772.4	1.52
Cu ₂ O-P25	465.9	2.52
Cu ₂ O maxed TiO ₂	978.4	1.20

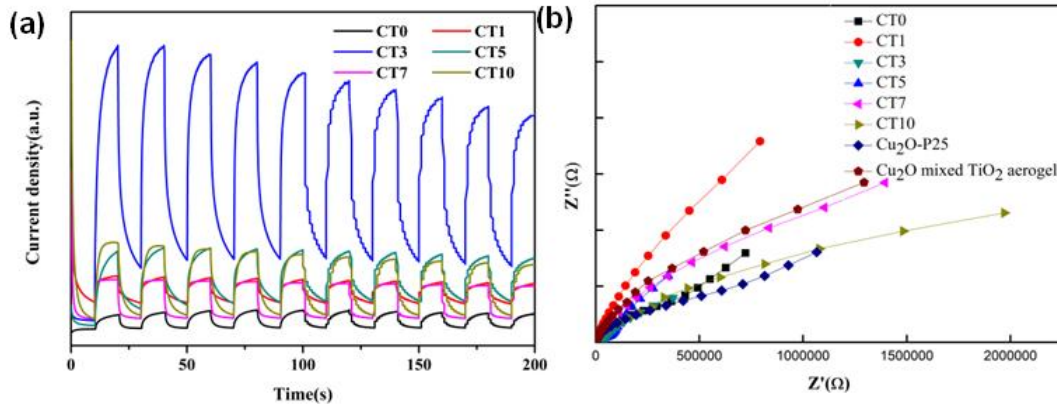


Fig. 8. Electrochemical test of the samples:(a) Nyquist plot, (b) Transient photocurrent density response of samples

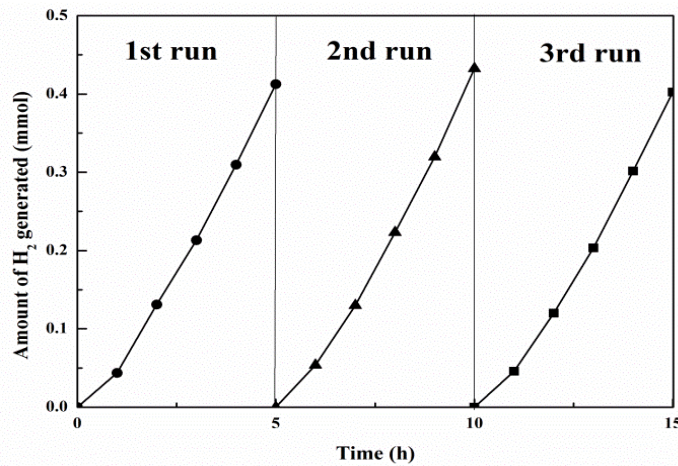


Fig. 9. Hydrogen production activity of the recycled photocatalyst (50 mg of the catalyst, 278 K) Cu_2O itself usually suffers from relatively poor photostability when used as a photocatalyst [18-22]

3.4 Reusability of the Recycled Photocatalysts

In order to confirm the reproducibility of H_2 production using Cu_2O -modified TiO_2 aerogel photocatalysts, three experiments were carried out at the same condition. The results were averaged and the average value of H_2 production is about $1.41 \text{ mmol}/(\text{g}\cdot\text{h})$. The results are displayed in Fig. 7. However, when Cu_2O was combined with TiO_2 aerogel, its photostability was significantly enhanced.

4. CONCLUSION

In summary, high-surface-area ($400\text{-}500 \text{ m}^2/\text{g}$) mesoporous of Cu_2O - TiO_2 aerogels with

relatively high concentration of Cu_2O were prepared and used in photocatalytic splitting of water under simulated solar light irradiation. Cu_2O - TiO_2 aerogel containing 3 wt% Cu_2O exhibited the highest hydrogen evolution rate of $1.40 \text{ mmol}/(\text{g}\cdot\text{h})$ which was about 33 and 9 times higher than those of pure TiO_2 aerogels ($0.043 \text{ mmol}/\text{g}\cdot\text{h}$) and Cu_2O -modified Degussa P25 titania ($0.15 \text{ mmol}/\text{g}\cdot\text{h}$). Moreover, the materials displayed good photocatalytic stability and long-term durability.

ACKNOWLEDGEMENTS

The authors thank the National Natural Science Foundation of China (22062026). The authors also thank The Yunling Scholar

(K264202012420), the Industrialization Cultivation Project (2016CYH04), the Key Projects for Research and Development of Yunnan Province (2018BA065), Key Laboratory of Advanced Materials for Wastewater Treatment of Kunming for financial support. The authors also thank Advanced Analysis and Measurement Center of Yunnan University for the sample testing service.

COMPETING INTERESTS

Authors have declared that no competing interests exist.

REFERENCES

1. Fujishima A, Honda K. Electrochemical Photolysis of Water at a Semiconductor Electrode. *Nature*. 1972;238:37-38.
2. Hoffmann MR, Martin ST, Choi W, Bahnemann DW. Environmental Applications of Semiconductor Photocatalysis. *Chem. Rev.* 1995;95:69-96.
3. Yu JG, Wang B. Effect of calcination temperature on morphology and photoelectrochemical properties of anodized titanium dioxide nanotube arrays; *Appl. Catal. B.* 2010;94:295-302.
4. Brian O'Regan, Michael Grätzel. A low-cost, high-efficiency solar cell based on dye-sensitized colloidal TiO₂ films. *Nature*. 1991;353:737-740.
5. Kraeutler B, Bard AJ. Photoelectrosynthesis of ethane from acetate ion at an n-type titanium dioxide electrode. The photo-Kolbe reaction. *J. Am. Chem. Soc.* 1977;99(23):7729-7731.
6. Nosaka Y, Koenuma K, Ushida K, Kira Langmuir A. Reaction Mechanism of the Decomposition of Acetic Acid on Illuminated TiO₂ Powder Studied by Means of in Situ Electron Spin Resonance Measurements. *Langmuir*. 1996;12(3):736-738.
7. Chen X, Mao SS. Titanium Dioxide Nanomaterials: Synthesis, Properties, Modifications, and Applications. *Chem. Rev.* 2007;107(7):2891-2959.
8. Jin ZL, Zhang XJ, Li YX, Li SB, Lu GX. 5.1% Apparent quantum efficiency for stable hydrogen generation over eosin-sensitized CuO/TiO₂ photocatalyst under visible light irradiation. *Catal. Commun.* 2007;8(8):1267-1273.
9. Gombac V, Sordelli L, Montini T, Delgado JJ, Adamski A, Adami G, Cargnello M, Bernal S, Fornasiero P. CuO_x-TiO₂ Photocatalysts for H₂ Production from Ethanol and Glycerol Solutions. *J. Phys. Chem. A*, 2010;114(11):3916-3925.
10. Park JH, Kim S, Bard AJ. Novel Carbon-Doped TiO₂ Nanotube Arrays with High Aspect Ratios for Efficient Solar Water Splitting. *Nano Lett.* 2006;6(1):24-28.
11. Zou ZG, Ye JH, Sayama K, Arakawa H. Direct splitting of water under visible light irradiation with an oxide semiconductor photocatalyst. *Nature*, 2001;414:625-627.
12. Ni M, Leung MKH, Leung DYC, Sumathy K. A review and recent developments in photocatalytic water-splitting using TiO₂ for hydrogen production. *Renew. Sust. Energy Rev.* 2007;11(3) 2007:401-425.
13. Nada A, Barakat MH, Hamed HA, Mohamed NR, Veziroglu TN. Studies on the photocatalytic hydrogen production using suspended modified TiO₂ photocatalysts. *Int. J. Hydrogen Energy*.2005;30(7):687-691.
14. Zhou MH, Yu JG, Liu SW, Zhai PC, Huang BB. Spray-hydrolytic synthesis of highly photoactive mesoporous anatase nanospheres for the photocatalytic degradation of toluene in air. *Appl. Catal. B.* 2009;89(1-2):160-166.
15. Walter MG, Warren EL, McKone JR, Boettcher SW, Mi QX. Solar Water Splitting Cells. *Santori EA, Lewis NS. Chem. Rev.* 2010;110(11):6446-6473.
16. He J, Chen DM, Li YL, Shao JL, Xie J, Sun YJ, Yan ZY, Wang JQ. Diatom-templated TiO₂ with enhanced photocatalytic activity: biomimetics of photonic crystals *Appl. Phys. A.* 2013;113:327-332.
17. Slamet HW, Nasution E, Purnama S, Kosela J. Gunlazuardi. Photocatalytic Reduction of CO₂ on Copper-doped Titania Catalysts Prepared by Improved-impregnation Method. *Catal. Commun.* 2005;6(5):313-319.
18. Bamwenda GR, Tsubota S, Nakamura T, Haruta M. Photoassisted hydrogen production from a water-ethanol solution: a comparison of activities of Au□TiO₂ and Pt□TiO₂. *J. Photochem. Photobiol. A*, 1995;89(2):177-189.
19. Sayama K, Arakawa H. Effect of carbonate salt addition on the photocatalytic decomposition of liquid water over Pt-TiO₂ catalyst. *J. Chem. Soc. Faraday Trans.* 1997;93: 1647-1654.

20. Sreethawong T, Yoshikawa S. Enhanced photocatalytic hydrogen evolution over Pt supported on mesoporous TiO₂ prepared by single-step sol-gel process with surfactant template. *Int. J. Hydrogen Energy*. 2006;31(6):786-796.
21. Zhang XH, Veikko U, Mao J, Cai P, Peng TY. Visible-Light-Induced Photocatalytic Hydrogen Production over Binuclear Rull-Bipyridyl Dye-Sensitized TiO₂ without Noble Metal Loading. *Chemistry*. 2012;18(38):12103-12111.
22. Chen WT, Jovic V, Waterhouse DS, Idriss H, Waterhouse GIN. The role of CuO in promoting photocatalytic hydrogen production over TiO₂. *Int. J. Hydrogen Energy*. 2013;38(35):15036-15048.
23. Hirano K, Suzuki E, Ishikawa A, Moroi T, Shiroishi H, Kaneko M. Sensitization of TiO₂ particles by dyes to achieve H₂ evolution by visible light. *J. Photo. Photo A*. 2000;136(3):157-161.
24. Pan L, Zou JJ, Wang SB, Huang ZF, Zhang XW, Wang L. Enhancement of visible-light-induced photodegradation over hierarchical porous TiO₂ by nonmetal doping and water-mediated dye sensitization. *Appl. Sur. Scif*. 2013;268(1):252-258.
25. Yu JG, Xiang QJ, H M. Zhou. Preparation, characterization and visible-light-driven photocatalytic activity of Fe-doped titania nanorods and first-principles study for electronic structures. *Appl. Catal. B*. 2009;90(3-4):595-602.
26. Kang MY, Yun HJ, Yu S., Kim W, Kim ND, Yi J. Effect of TiO₂ crystalline phase on CO oxidation over CuO catalysts supported on TiO₂. *J. Mol. Catal. A:Chem*. 2013;368-369:72-77.
27. Liu Y, Zhang B, Luo L, Chen X, Wang Z, Wu E, Su D, Huang W. TiO₂/Cu₂O Core/Ultrathin Shell Nanorods as Efficient and Stable Photocatalysts for Water Reduction. *Angew. Chem. Int. Ed*. 2015;54(50):15260-15265.
28. Wang M, Sun L, Lin Z, Cai J, Xie K, Lin C. p-n Heterojunction photoelectrodes composed of Cu₂O-loaded TiO₂ nanotube arrays with enhanced photo electrochemical and photoelectrocatalytic activities. *Energy Environ. Sci*. 2013;6:1211-1220.
29. Bandara J, Udawattab CPK, Rajapakse a CSK. Highly stable CuO incorporated TiO₂catalyst for photocatalytic hydrogen production from H₂O. *Photochem Photobiol Sci*. 2005;11: 857-861.
30. Yu JG, Hai Y, Jaroniec M. Photocatalytic hydrogen production over CuO-modified titania. *J.Colloid, Interf. Sci*. 2011;357(1):223-228.
31. Wei TY, Lu SY, Chang YC. Transparent, Hydrophobic Composite Aerogels with High Mechanical Strength and Low High-Temperature Thermal Conductivities. *J. Phys. Chem. B*. 2008;112(38):11881-11886.
32. Chia-Chien Lin, Te-Yu Wei, Kuan-Ting Lee and Shih-Yuan Lu. Titania and Pt/titania aerogels as superior mesoporous structures for photocatalytic water splitting. *J. Mater. Chem*. 2011;21:12668.
33. Wei T Y, Chen CH, Chien HC, Lu SY, Hu CC. A Cost-Effective Supercapacitor Material of Ultrahigh Specific Capacitances: Spinel Nickel Cobaltite Aerogels from an Epoxide-Driven Sol-Gel Process. *Adv. Mater*. 2010;22(3):347-351.
34. Anastasescu C, Spataru N, Culita D, Atkinson I, Spataru T, Bratan V, Munteanu C, Anastasescu M, Negriila C, Balint I. Chemically assembled light harvesting CuO_x-TiO₂ p-n heterostructures. *Chem. Eng. J*. 2015;281(1):303-311.
35. Kumar DP, Reddy NL, Srinivas B, Durgakumari V, Roddatis V, Bondarchuk O, Karthik M, Ikuma Y, Shankar MV. Stable and active Cu_xO/TiO₂ nanostructured catalyst for proficient hydrogen production under solar light irradiation. *Sol Energy Mater Sol Cells*. 2016;146:63-71.
36. Wang J, Uma S, Klabunde KJ. Visible light photocatalysis in transition metal incorporated titania-silica aerogels. *Appl. Catal. B*. 2004;48(2):151-154.
37. Yu J, Hai Y, Jaroniec M. Photocatalytic hydrogen production over CuO-modified titania. *J. Colloid Interface Sci*. 2011;357(1):223-228.
38. Lalitha K, Sadanandam G, Kumari VD, Subrahmanyam M, Sreedhar B, Hebalkar NY. Highly Stabilized and Finely Dispersed Cu₂O/TiO₂: A Promising Visible Sensitive Photocatalyst for Continuous Production of Hydrogen from Glycerol:Water Mixtures. *J. Phys. Chem. C*, 2010;114(50):22181-22189.
39. Chiarello GL, Dozzi MV, Sellì E. TiO₂-based materials for photocatalytic hydrogen production. *J. Energy Chem*. 2017;26(2):250-258.

40. Tamiolakis I, Papadas IT, Spyridopoulos KC, Armatas GS. Mesoporous assembled structures of Cu₂O and TiO₂ nanoparticles for highly efficient photocatalytic hydrogen generation from water. RSC Adv. 2016;6:54848-54855.

© 2021 Jiang et al.; This is an Open Access article distributed under the terms of the Creative Commons Attribution License (<http://creativecommons.org/licenses/by/4.0>), which permits unrestricted use, distribution, and reproduction in any medium, provided the original work is properly cited.

Peer-review history:
The peer review history for this paper can be accessed here:
<https://www.sdiarticle4.com/review-history/70839>